PREPARATION OF ORGANIZED MESOPOROUS SILICA FROM SODIUM METASILICATE SOLUTIONS IN ALKALINE MEDIUM USING NONIONIC SURFACTANTS

Markéta ZUKALOVÁ[1,*], Jiří RATHOUSKÝ[2] and Arnošt ZUKAL[3]

J. Heyrovský Institute of Physical Chemistry, Academy of Sciences of the Czech Republic, 182 23 Prague 8, Czech Republic; e-mail: [1] marketa.zukalova@jh-inst.cas.cz, [2] jiri.rathousky@jh-inst.cas.cz, [3] arnost.zukal@jh-inst.cas.cz

Received May 27, 2003
Accepted July 24, 2003

A new procedure has been developed, which is based on homogeneous precipitation of organized mesoporous silica from an aqueous solution of sodium metasilicate and a nonionic poly(ethylene oxide) surfactant serving as a structure-directing agent. The decrease in pH, which induces the polycondensation of silica, is achieved by hydrolysis of ethyl acetate. Owing to the complexation of Na^+ cations by poly(ethylene oxide) segments, assembling of the mesostructure appears to occur under electrostatic control by the $S^0Na^+I^-$ pathway, where S^0 and I^- are surfactant and inorganic species, respectively. As the complexation of Na^+ cations causes extended conformation of poly(ethylene oxide) segments, the pore size and pore volume of organized mesoporous silica increase in comparison with materials prepared under neutral or acidic conditions. The assembling of particles can be fully separated from their solidification, which results in the formation of highly regular spherical particles of mesoporous silica.

Keywords: Mesoporous SiO_2; Silicates; Nonionic surfactants; Sodium metasilicate; Homogeneous precipitation; Spherical morphology; Heterogeneous catalysis.

In recent years, the use of nonionic surfactants as structure-directing agents has led to the development of a new class of organized mesoporous silicas (OMSs). Those synthesized with oligomeric alkyl- or alkyl-aryl-poly(ethylene oxide) (PEO) surfactants and with poly(alkylene oxide) block copolymers exhibit a number of advantages over the more traditional M41S silica family, offering new pore topologies and feasible techniques for controlling the pore size from 5 to 30 nm. Additionally, nonionic surfactants are easy to remove from the as-made material, they are relatively inexpensive, environmentally compatible and biodegradable, which makes them much more attractive structure directors than the toxic long-chain ammonium surfactants used in the syntheses of the M41S silicas.

Considerable effort has been aimed at expanding this new class of OMS by testing different synthetic pathways based on different silicon sources and reaction mechanisms. Early attempts employed tetraethyl orthosilicate (TEOS) as the inorganic precursor. Bagshaw *et al.*[1] used alkyl- and alkyl-aryl-PEO surfactants in aqueous solutions to synthesize wormhole-like mesoporous silica in neutral medium, demonstrating the feasibility of assembling OMS by taking the neutral S^0I^0 pathway, *i.e.* by hydrogen bond interactions between the non-charged surfactant (S^0) and the neutral inorganic species (I^0). Later on, Zhang *et al.*[2] showed the practicability of the $(S^0M^{n+})I^0$ reaction pathway at near-neutral pH, in which hydrogen bonds are formed between a cationic metal complex form of a nonionic PEO surfactant and electrically neutral inorganic precursor. The complexation of small metal cations M^{n+} (such as Li^+, Co^{2+}, Ni^{2+}, *etc.*) by the OCH_2CH_2 groups of PEO surfactants brings the assembly process under electrostatic control. The OMSs prepared in this way were characterized by a long-range framework order. Zhao *et al.*[3,4] reported the preparation of OMS under strongly acidic conditions. Below the aqueous isoelectric point of silica, cationic silica species are present as precursors and the electrostatic assembling occurs through intermediate $(S^0H^+)(X^-I^+)$, where X^- and I^+ denote the halide anion and a protonated Si-OH moiety, respectively. Highly ordered mesoporous silica structures prepared using alkyl-PEO oligomeric surfactants and poly(alkylene oxide) block copolymers include cubic, three-dimensional hexagonal, two-dimensional hexagonal, and lamellar mesostructures denoted as the SBA family. Owing to its capability of pore size adjustment and tailored particle morphology, the SBA-15 with a two-dimensional hexagonal (P6mm) structure is currently the most prominent member of the family of nonionic surfactant-templated materials.

As tetraalkyl orthosilicates are not economically viable silica sources, their replacement by inexpensive sodium silicate solutions has been recently attempted. Kim and Stucky[5] reported the synthesis of highly ordered mesoporous silicas under strongly acidic conditions, various members of the SBA family being obtained depending on the type of block copolymer used. Kim *et al.*[6,7] developed a procedure based on PEO surfactants as the structure directors under neutral conditions. This assembly provided either OMS with a wormhole porous structure[6] or highly ordered materials analogous to the SBA family[7]. Sierra *et al.*[8] reported the preparation of OMS from sodium silicate in the presence of alkyl-aryl-PEO surfactant Triton X100 at pH between 3 and 10.5. They suggested the formation of ionic bonds $S^0Na^+I^-$ as the assembling mechanism at pH higher than 8. However, the removal of the surfactant by calcination at 600 °C led either to an extensive

restructuring of the silica framework or to the formation of a completely amorphous material. More recently, Sierra *et al.*[9] prepared OMS with controlled morphology from sodium silicate and Triton X100 at pH between 2 and 6.

In addition to the mentioned one-step procedures, also double-step pathways have been developed, in which the assembling and polymerization steps are separated[10–13]. First, a dilute solution of surfactant and silica precursor (TEOS or sodium silicate) is stabilized at pH of 2–4. Afterwards, the silica condensation is induced by adding a small amount of sodium fluoride or by increasing pH. The main advantage of the double-step procedure is the simple control of pore size, pore volume and particle morphology by temperature[10] or pH (ref.[13]) of the reaction mixture. For example, OMS with spherical particles with mean size of 7 μm and with narrow size distribution was prepared from TEOS and alkyl-PEO surfactant Tergitol 15S12 (ref.[11]).

In recent years, we have developed a synthetic protocol for homogeneous precipitation of OMS from sodium metasilicate in alkaline medium with a quaternary alkylammonium surfactant as a structure director[14,15]. The decrease in pH of the reaction mixture from the starting value of ≈11, which induces the polycondensation of the silica, is achieved by the hydrolysis of a suitable ester of acetic acid. A precise control of pH allowed preparation of OMS with different structure features. Here we report a synthesis protocol, which combines the advantages of both the homogeneous precipitation of OMS from aqueous sodium metasilicate and the use of nonionic surfactants. As the assembling of mesostructure takes place in alkaline medium without initial acidification of the reaction mixture, this study completes the spectrum of methods for the synthesis of OMS with nonionic surfactants as structure directing agents.

EXPERIMENTAL

Materials

Sodium metasilicate (Na_2SiO_3), ethyl acetate (EtOAc) and surfactant Brij 56 were purchased from Aldrich, surfactant Tween 60 from Fluka. Triblock copolymers Pluronic PE9400 and P123 were obtained from BASF, Germany and BASF, U.S.A., respectively.

The abbreviated formulae of surfactants used are listed in Table I.

Synthesis

The reaction mixture was prepared in a poly(methylpentene) (Nalgene) bottle placed in a water thermostat. Surfactant (1 g) followed by Na_2SiO_3 (2.5 g) was dissolved in distilled water (900 ml) at temperature given in Table I, resulting in a clear solution. Synthesis with

Pluronic P123 was performed at 35 °C since the reaction mixture became opaque at higher temperature. Afterwards, EtOAc (5 ml) was added under stirring, which was finished after 20 s, followed by aging at synthesis temperature (Table I) for 24 h. With sample B56/A, however, the stirring was continued during this aging. Finally, all the samples were aged at 90 °C for 48 h.

The resulting solid product was recovered by hot filtration, washed with distilled water followed by ethanol, and dried at ambient temperature. The surfactant was removed by calcination at 600 °C (2 °C/min) under flowing air for 12 h.

Characterization

Adsorption isotherms of nitrogen at 77 K were measured with a Micromeritics ASAP 2010 instrument. Before the adsorption measurement, all the samples were degassed at 300 °C until a pressure of 0.1 Pa was attained. The BET surface area S_{BET} was evaluated from adsorption data in the relative pressure range from 0.05 to 0.25. The total mesopore volume V_{ME} was determined from the amount adsorbed at a relative pressure of about 0.99. The mesopore size distribution was calculated from the desorption branch of the isotherm using the BJH method[16].

Powder X-ray diffraction (XRD) patterns were collected on a Siemens D 5005 diffractometer in the Bragg–Brentano geometry arrangement with CrKα radiation. (The CrKα radiation of the wavelength of 0.2290 nm is more suitable for the study of solids with a long-range ordering than the CuKα radiation of the wavelength of 0.1541 nm.) Scanning

TABLE I
OMS samples and their structural parameters

Code[a]	Surfactant	t, °C	S_{BET} $m^2\ g^{-1}$	V_{ME} $cm^3\ g^{-1}$	D_{ME}, nm
B56	Brij 56, $C_{16}H_{33}(EO)_{10}$	75	540	1.733	10.4
B56/A[b]	Brij 56, $C_{16}H_{33}(EO)_{10}$	75	334	0.808	9.1
B56/B	Brij 56, $C_{16}H_{33}(EO)_{10}$	55	482	0.960	8.3
PE9400	Pluronic PE9400, $(EO)_{20}(PO)_{50}(EO)_{20}$[c]	75	451	1.053	8.4
P123	Pluronic 123, $(EO)_{20}(PO)_{70}(EO)_{20}$	35	547	1.016	7.0
Tw60	Tween 60, poly(oxyethylene) sorbitan monostearate[d]	75	415	1.632	7.9

[a] Samples of organized mesoporous silica are designated by abbreviations of the surfactant used. [b] Aged with stirring. [c] PO denotes propylene oxide unit. [d] Twenty oxyethylene groups are randomly distributed over the four available sites. t, synthesis temperature; S_{BET}, BET surface area; V_{ME}, mesopore volume; D_{ME}, mesopore diameter corresponding to the maximum of the distribution curve.

electron microscopy (SEM) was performed using a JEOL JSM-5500LV microscope at accelerating voltage 9 kV. Transmission electron microscopy (TEM) was carried out on a Philips CM30T instrument with a LaB_6 source of electrons at accelerating voltage 300 kV. Samples were mounted on a Quantifoil microgrid carbon polymer supported on a copper grid by evaporating a few droplets of ethanolic suspension of ground sample.

RESULTS

The optimization of the reaction mixture composition has shown that well-organized materials are obtained exclusively from dilute reaction mixtures. When the concentration was raised to the level used in the synthesis in an acidic medium, *i.e.* increased 44 times[5], only non-organized silica gel was formed, which is obviously due to too fast non-organized polycondensation in comparison with the mesostructure assembly at high concentrations of silicate anions.

The rate of pH decrease of the reaction mixture practically does not depend on the surfactant used. Figure 1 gives a typical curve of the time evolution of pH after the addition of EtOAc. The horizontal bars mark the boundaries of the region between pH 8.5 and 9.0, in which clear reaction mixture becomes opaque due to the formation of solid particles.

OMSs Prepared with Brij 56

Nitrogen isotherms on samples B56 and B56/A are characterized by the type H2 hysteresis loop with relatively steep adsorption and desorption branches

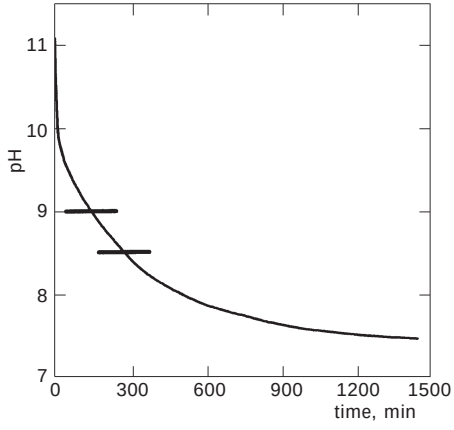

FIG. 1
Time evolution of pH of the reaction mixture. The horizontal bars mark the region, in which solid phase begins to form

(Fig. 2)[17]. The isotherm on B56/B is very similar to that on B/56A. The BET surface areas and mesopore volumes of samples B56, B56/A and B56/B are given in Table I. As the pore size distribution of these samples is unimodal and symmetrical (Fig. 3), the mean mesopore diameter D_{ME} corresponds to the maximum of the pore size distribution (Table I).

The TEM image of the most dispersed sample B56 shows a wormhole-like pore structure (Fig. 4), which is in agreement with the XRD pattern exhibit-

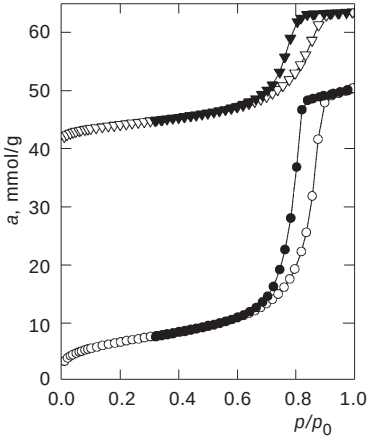

FIG. 2
Nitrogen adsorption isotherms on samples B56 (○) and B56/A (▽). The isotherm on B56/A is shifted by 40 mmol/g. Solid points denote desorption

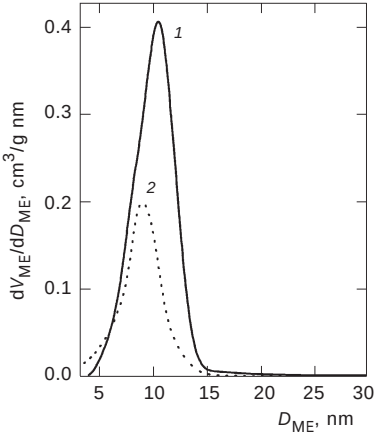

FIG. 3
Pore size distribution for samples B56 (*1*) and B56/A (*2*)

ing only one reflection (Fig. 5). The position of the maximum of this reflection corresponds to the pore–pore correlation distance of ≈11.5 nm (ref.[6]). The pore wall thickness, assessed by subtracting the pore diameter 10.4 nm (Table I) from the correlation distance, equals ≈1.1 nm.

The SEM image of sample B56 (Fig. 6) shows highly regular spherical particles 5 μm in diameter. Stirring the reaction mixture during the aging was found to disturb the assembling process. For example, sample B56/A, whose reaction mixture was stirred during its aging at 75 °C, is of much worse quality than sample B56 (Figs 2 and 3, Table I), being characterized by reduced surface area and pore volume, and also irregular particle morphology (Fig. 7).

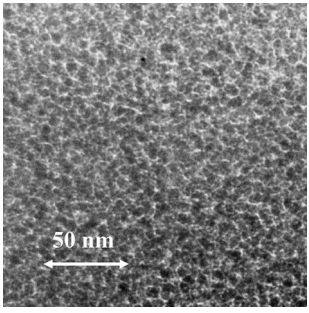

FIG. 4
Transmission electron micrograph of sample B56

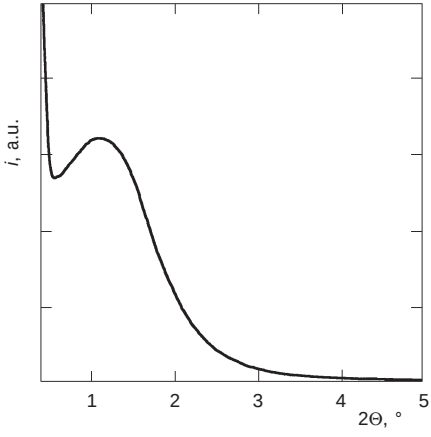

FIG. 5
X-Ray diffraction pattern of sample B56

OMSs Prepared with Pluronic PE9400, Pluronic P123 and Tween 60

Adsorption isotherms of samples PE9400 and P123 (Fig. 8), calculated structure data (Table I) and pore size distributions (Fig. 9) clearly show their similarity. The somewhat smaller mesopore diameter of sample P123 is probably due to the lower synthesis temperature, which is a general feature of OMS, prepared using nonionic surfactants[4,6,10].

The nitrogen isotherm of sample Tw60 and calculated structure data are given in Fig. 8 and Table I. As distinct from the acidic pathway, which affords a well-ordered mesoporous silica with Tween 60 (refs[4,13]), the pore size distribution of sample Tw60 exhibits a broad peak tailing off towards larger pore diameters (Fig. 9). Hence, this sample is characterized by a poorly ordered mesoporous structure, which is confirmed by the absence of reflections in its XRD pattern.

SEM images (not shown) of samples PE9400, P123 and Tw60 revealed bead-like particles with size ranging from 3 to 6 μm.

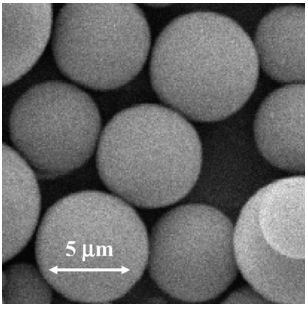

FIG. 6
Scanning electron micrograph of sample B56

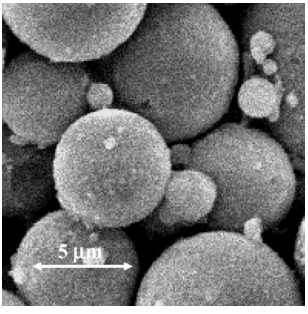

FIG. 7
Scanning electron micrograph of sample B56/A

DISCUSSION

Occurring in an alkaline medium and using sodium metasilicate as the silica source, the assembling of OMS presented in this study can be postulated to follow exclusively the $S^0Na^+I^-$ reaction pathway.

Pore size and volume of sample B56 (10.4 nm, 1.73 cm^3/g) are much larger than those of SBA-15 prepared from TEOS under strongly acidic conditions (3.5 nm, 1.02 cm^3/g)[4] or OMS obtained from sodium silicate under

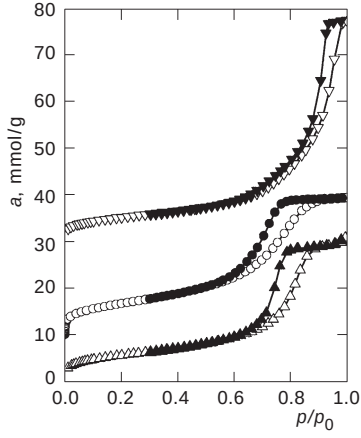

FIG. 8

Nitrogen adsorption isotherms of samples PE9400 (△), P123 (○) and Tw60 (▽). The isotherms of P123 and Tw60 are shifted by 10 and 30 mmol/g, respectively. Solid points denote desorption

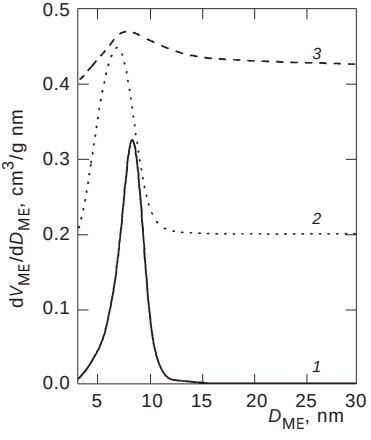

FIG. 9

Pore size distribution for samples PE9400 (*1*), P123 (*2*) and Tw60 (*3*). The distribution curves for samples P123 and Tw60 are shifted by 0.2 and 0.4 cm^3/g nm, respectively

neutral conditions (5.0 nm, 0.90 cm^3/g)[6], which reveals the specificity of the $S^0Na^+I^-$ reaction pathway. The pore size and pore volume of OMS prepared in this way increase because the complexation of Na^+ cations with the PEO segments causes their extended conformation. The pore ordering of sample B56 is less regular than that of the SBA-15 silica, being similar to that of the OMS prepared under neutral conditions.

Due to weak interactions between silicate anions and the surfactant, stirring the reaction mixture during aging disturbs the assembling process. Generally the stirring should impede any synthesis following the $S^0Na^+I^-$ pathway. For example, sample B56/A, whose reaction mixture was stirred during aging at 75 °C, is of much worse quality than sample B56 (Figs 2 and 3, Table I), characterized by reduced surface area and pore volume, and also irregular particle morphology (Fig. 7).

With sample B56, the assembling was fully separated from the polycondensation. First, soft particles containing low molecular weight silica oligomers were formed. Owing to the effect of surface tension, they acquired the spherical shape, which was preserved even after the solidification due to the silica polycondensation induced by the pH decrease. Because of the lower synthesis temperature, the solidification of soft particles of sample B56/B was delayed, which makes it possible to observe their coalescence (Fig. 10). This phenomenon confirms the originally liquidlike nature of assembled particles.

SBA-15, prepared using TEOS and Pluronic P123 and aged at similar temperature as sample P123, exhibits a surface area of 920 m^2/g which is substantially larger than that of P123 (547 m^2/g)[4]. This difference is obviously due to the presence of micropores in SBA-15. As micropores are filled with nitrogen molecules at equilibrium pressures below the lower limit of the BET equation validity, the BET monolayer capacity comprises both the ca-

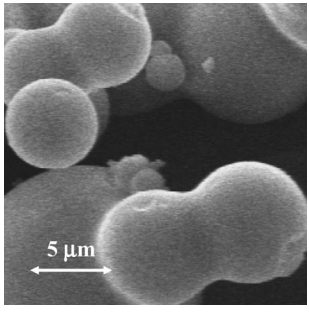

FIG. 10
Scanning electron micrograph of sample B56/B

pacity of the monolayer on the mesopore surface and the amount a_{MI} (mmol/g) of nitrogen, which fills the micropore volume V_{MI} (cm^3/g):

$$a_{MI} = V_{MI}/\nu_m \,, \qquad (1)$$

where $\nu_m = 0.0348$ $cm^3/mmol$ is the molar volume of liquid nitrogen at 77 K. (The BET method can be formally applied to nitrogen isotherms on micro-mesoporous materials provided that the micropore filling contribution to the total amount adsorbed is not significant.) The apparent surface area S_{APP} (m^2/g) corresponding to the micropores is

$$S_{APP} = L\sigma a_{MI} = L\sigma V_{MI}/\nu_m = 2804\ V_{MI} \,, \qquad (2)$$

where L is the Avogadro constant and $\sigma = 0.162$ nm^2 is the average area occupied by each nitrogen molecule. As the volume of micropores of SBA-15, assessed using the α_s-method, ranges from 0.08 to 0.12 cm^3/g, the corresponding apparent surface area S_{APP} calculated by Eq. (*2*) equals 224–336 m^2/g (ref.[18]). Taking into account the presence of micropores, an approximate agreement between the surface areas of SBA-15 and P123 is achieved.

The absence of micropores in sample P123 can be evidenced by means of a high-resolution α_s plot. Figure 11 shows the low-pressure region of this plot, constructed using the standard adsorption data obtained by Jaroniec

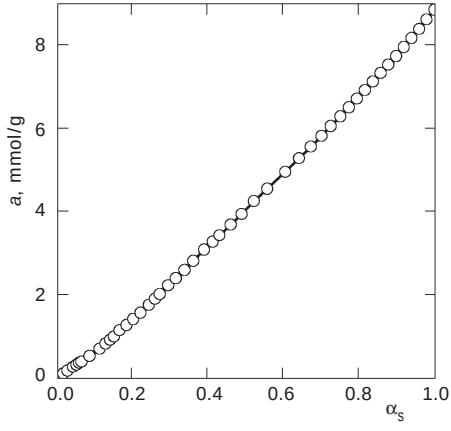

FIG. 11
Initial part of the α_s plot for sample P123

et al.[19] on non-porous silica. Since this plot is slightly convex to the α_s axis, there is no micropore filling contribution to the amount adsorbed on the mesopore surface. The slight deviations from linearity are probably due to different surface chemical structures.

Tween 60 is characterized by a short hydrophobic chain and a large hydrophilic head consisting of three free PEO chains and one linking the ring to the hydrophobic tail. Similarly to both Pluronics, PEO chains of Tween 60 consist of ≈20 oxyethylene units altogether, which are, however, randomly distributed over four segments. Because of the special shape of its molecule, Tween 60 is not suitable for assembling a well-ordered mesostructure by the $S^0Na^+I^-$ reaction pathway. Nevertheless, it does contribute to the formation of the silica mesophase since experiments performed without any surfactant in the reaction mixture gave no solid product.

CONCLUSIONS

Organized mesoporous silicas were synthesized in alkaline medium from sodium metasilicate using oligomeric alkyl-PEO surfactants or triblock poly(alkylene oxide) copolymers as structure directors. The assembly occurred by the $S^0Na^+I^-$ pathway, wherein electrostatic forces are introduced through PEO complexation of sodium cations.

The specific features of the synthesis in alkaline media make it possible to obtain OMS with differing structure properties in comparison with those obtained in neutral or acidic media. As the complexation of Na^+ cations with the PEO segments causes their extended conformation, the pore size and pore volume of OMSs are enhanced. The structural ordering of OMSs prepared in alkaline medium is less regular than that of analogous materials synthesized under strongly acidic conditions, being similar to structural ordering of silicas prepared under neutral conditions.

The assembling of particles was fully separated from their solidification due to polycondensation. If oligometric alkyl-PEO surfactant Brij 56 was used as the structure director, highly regular spherical particles 5 μm in diameter were prepared.

In comparison with materials prepared under acidic conditions, OMSs obtained in this study are purely mesoporous materials. This feature could be advantageous with respect to their potential applications as adsorbents and supports in catalysis.

The authors thank Patricia J. Kooyman (National Center for High Resolution Electron Microscopy, Delft University of Technology, Delft, Netherlands) for taking the TEM images.

REFERENCES

1. Bagshaw S. A., Prouzet E., Pinnavaia T. J.: *Science* **1995**, *269*, 1242.
2. Zhang W., Glomski B., Pauly T. R., Pinnavaia T. J.: *Chem. Commun.* **1999**, 1803.
3. Zhao D., Feng J., Huo Q., Melosh N., Fredrickson G. H., Chmelka B. F., Stucky G. D.: *Science* **1998**, *279*, 48.
4. Zhao D., Huo Q., Feng J., Chmelka B. F., Stucky G. D.: *J. Am. Chem. Soc.* **1998**, *220*, 6024.
5. Kim J. M., Stucky G. D.: *Chem. Commun.* **2000**, 1159.
6. Kim S.-S., Pauly T. R., Pinnavaia T. J.: *Chem. Commun.* **2000**, 835.
7. Kim S.-S., Pauly T. R., Pinnavaia T. J.: *Chem. Commun.* **2000**, 1661.
8. Sierra L., Guth J.-L.: *Microporous Mesoporous Mater.* **1999**, *27*, 243.
9. Sierra L., Lopez B., Guth J.-L.: *Microporous Mesoporous Mater.* **2000**, *39*, 519.
10. Prouzet E., Pinnavaia T. J.: *Angew. Chem., Int. Ed. Engl.* **1997**, *36*, 516.
11. Boissiere C., van der Lee A., El Mansouri A., Larbot A., Prouzet E.: *Chem. Commun.* **1999**, 2047.
12. Boissière C., Larbot A., Prouzet E.: *Chem. Mater.* **2000**, *12*, 1937.
13. Boissière C., Larbot A., van der Lee A., Kooyman P. J., Prouzet E.: *Chem. Mater.* **2000**, *12*, 2902.
14. Schulz-Ekloff G., Rathouský J., Zukal A.: *Microporous Mesoporous Mater.* **1999**, *27*, 273.
15. Schulz-Ekloff G., Rathouský J., Zukal A.: *J. Inorg. Mater.* **1999**, *1*, 97.
16. Barrett E. P., Joyner L. G., Halenda P. P.: *J. Am. Chem. Soc.* **1951**, *72*, 373.
17. Rouquerol F., Rouquerol J., Sing K.: *Adsorption by Powders and Porous Solids*, pp. 171, 204. Academic Press, London 1999.
18. Kruk M., Jaroniec M., Ko C. H., Ryoo R.: *Chem. Mater.* **2000**, *12*, 1961.
19. Jaroniec M., Kruk M., Olivier J. P.: *Langmuir* **1999**, *15*, 5410.